CHAPTER 26

Processing Monosized Powders

E. BARRINGER, N. JUBB, B. FEGLEY, R. L. POBER, AND H. K. BOWEN

INTRODUCTION

Ceramic materials offer a nearly infinite variety of possible physicochemical characteristics which are controlled by the atomic structure and by the micro- and macrostructure. These materials are desired for their refractoriness, inertness, and special electronic, structural, and thermal properties. The chemical composition, phase composition and distribution, composition gradients, grain size, and other factors all contribute to the actual properties and performance, yet these parameters are difficult to control. Thus, the enormous potential of ceramic materials is met in only a few cases, and in this sense, *ceramics are materials of promise, not commerce.*

It is now widely accepted that in the case of high performance ceramics (those manufactured with high added value, for exacting performance), the problem lies in inadequate manufacturing technology. Microstructures and macrostructures cannot be controlled. In short, ceramics cannot be manufactured with high reliability and reproducibility largely because there is no underpinning science.[1] Since ceramic components formed by powder processing begin with more than 10^{12} particles, the problem of process control is exacerbated. From numerous discussions with ceramic manufacturers, the cost of this inadequacy can be determined for a large portion of the current $4 billion high performance ceramics business (see Table 26.1). For simplicity, we have divided the sequential ceramic powder processing operation into five items (Table 26.2). The approximate percentage of current manufacturing cost assignable to each item is also shown. Depending on the ceramic component being manufactured, the cost of rejection (note that this is not the percentage of components rejected) is about 50% (±25%) of the total manufacturing cost.

In *Ultrastructure Processing of Ceramics, Glasses, and Composites* (1984), L. L. Hench and D. R. Ulrich, Eds. John Wiley and Sons, New York.

Table 26.1 1980 High Technology Ceramics Markets[a]

Product	Japanese Sales ($ million)	Worldwide Sales ($ million)
Ceramic powders	130	250
Electronic IC packages/substrates	540	880
Capacitors	325	750
Piezoelectrics	145	195
Thermistor/varistors	125	200
Ferrites	380	480
Gas/humidity sensors	5	45
Translucent ceramics	20	45
Cutting tools	125	1025
Structural ceramics	120	250
Totals	1,915	4,120

[a] Taken from Ref. 2.

Traditionally, studies of ceramics processing centered on sintering and grain growth. These final steps in the process have been the most modelled and most studied topic since the early studies of Kuczynski.[3] Even though there were numerous investigations into solid state sintering mechanisms, technology still has relied on sintering aids and grain growth control additives.[4] Indeed, most commercial products are processed using liquid phase formers. In this respect, processing science seems doomed to empiricism as the search for additives continues.

Another important historical point is the oft observed phenomenon (and associated microstructural feature) that occurs in the very early stages of the typical sintering cycle for commercial powders, associated with agglomerated regions within the starting green microstructure. The agglomerates of densely packed particles sinter very rapidly; the grains coarsen, and these become the particles for the continuing (usually slow) sintering process.[5]

Table 26.2 Typical Manufacturing Costs for High Value Added Ceramics

1. Raw materials (powders, chemicals, etc.)	15%
2. Part shaping (mixing, milling, casting, etc.)	15%
3. Firing (binder burnout, sintering, etc.)	15%
4. Finishing (simple grinding, joining, etc.)	5%
5. Rejection at any step (1–4)	50%[a]

[a] The cost of rejection varies from product to product, but is generally in the range of 25–75% of the manufacturing cost.

The realization that the scaling laws for the sintering model indicate that 100 Å powders will sinter 10^6–10^8 times faster than micron size powders,[6] led the sintering specialists to desire powders that are not calcined or milled, but rather very fine powders produced by any of several methods (e.g., chemical synthesis).[7] These powders, which are often agglomerates of particles in the 100 Å range, can be readily densified, but the predicted advantage on the sintering time and temperature has not been generally realized. Rhodes[8] performed an enlightening study using alkoxide derived powders developed by Mazdiyasni and coworkers[7] and found that by dispersing the powders and eliminating agglomerates, dense green bodies could be centrifugally cast. These casts sintered to near theoretical density at very low temperatures (1100°C as opposed to 1700°C for calcined and milled powders).

We suggest that the major contributor to the cost of rejection is that current processing methods using conventional powders produce ceramic green bodies that are inhomogeneously packed, and thus the sintering process is difficult to control without additives. In fact, the liquid phase sintering aids[9] commonly used have the *primary* function of causing *particle rearrangement,* rather than increasing diffusive transport. The characteristics of liquid phase sintering aids (particulates are soluble in and wetted by the liquid) allow them to dissolve the necks between agglomerated particles and, under the action of capillary forces, to pull the structure into a more uniform spatial distribution of the particles. Similarly, Cannon[10] stated that the applied pressure during hot pressing performs the same function (rearranging the particles to give a more uniformly packed structure). Therefore, hot pressing usually results in more uniform microstructures and higher sintered densities at lower temperatures and shorter times.

The final guide to understanding controlled powder processing comes from insight into the competing processes of particle coarsening and pore removal (densification), and the need to maintain pores at grain boundaries for complete densification. This was discussed extensively by the MIT group[11] and resulted in a qualitative paradigm for powder processing that incorporates the observations stated above. For processing single-phase ceramics (no liquid forming additives) to high densities and with control of the microstructure at all stages of densification, one desires (1) an unagglomerated powder of monosized particles, 1 μm or less in size,* (2) the green microstructure to have a uniform distribution of the void space (pores) and as many particle-particle contacts as possible (approaching that for close-packing), and (3) the selection of the thermochemical variables (T, P, and composition) such that densification rather than particle coarsening occurs and that pores are pinned to grain boundaries (see Table 26.3).

* In most cases, the ideal powder is monosized and between 0.1 and 1.0 μm. This size provides enough surface free energy for sintering, yet not too much surface area to cause problems in highly loaded dispersions and problems with the adsorption and desorption of gases from the powder surface.

Table 26.3 Guidelines for Preparation of Oxide Ceramics

CHOICE OF GRAIN GROWTH INHIBITOR
1. Solute should decrease grain boundary mobility:
a. Soluble in host lattice.
b. Ionic size about the same.
c. Aliovalent.
d. If the host lattice is an insulator, the solute should not readily create electronic carriers.
2. Solute should not decrease pore mobility.
CHOICE OF SOLID STATE SINTERING AID
1. Solute should increase bulk or lattice diffusivity of slowest ion.
a. Soluble in host lattice.
b. Aliovalent.
2. Solute should decrease surface and vapor phase transport.

WHY PROCESS MONOSIZED POWDERS?

Unagglomerated powders with a very narrow size distribution have enormous potential in advancing the science of ceramics processing: (1) they represent experimental systems for which theoretical models can be derived and tested using observations of the total processing cycle; (2) given quantitative expressions, it is possible to scale the process, and thus the principles (and models) have technological value; (3) monosized powders are more readily characterized,* allowing the development of real time process control; and (4) monosized powders may have intrinsic processing advantages that make them of commercial importance.

An example of the processing advantage of powders with a narrow size distribution is shown in Fig. 26.1; the problems of coarsening and grain growth with powders having a wide size distribution are illustrated. Inasmuch as excess surface free energy is the driving force for both densification and coarsening, the large size distribution typical of comminution tends to make the small particles dissolve into the larger ones, and allows grain boundaries to pull away from pores.

Yet another example of the intrinsic advantage of monosized, unagglomerated powders is the schematic in Fig. 26.2. Single-sized particles with an

* Two examples are: (1) for theoretical reasons, spherical particles are easy to study by light scattering; and (2) monosized particles can be made to form ordered dispersions, which can be studied by light diffraction.

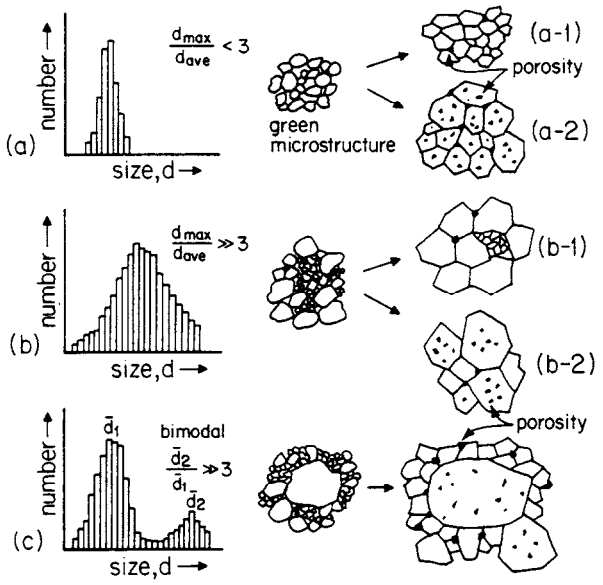

Figure 26.1 Schematic representation of the effects of powder size distribution on the sintered microstructure. For example, in (a-1), with a narrow size distribution and control of the grain boundary-pore interaction, dense sintered ceramics with the grain size slightly larger than the particle size are possible.

adequate repulsive force can be formed into concentrated slurries without flocs, and in some cases ordered dispersions are formed.[12] Recent theoretical studies [13] suggest that stability of dispersions against coagulation is very sensitive to the size distribution.

From this background information, we state two postulates that we believe will improve the manufacturability of high value added ceramics:

Postulate 1. Monosized particles are easier to process into uniform green microstructures (uniformity of the size and distribution of the voids), which results in easier control of the microstructure during densification.

Postulate 2. Submicron particles require modification of the interparticle forces by controlling the surface chemistry (usually in a liquid phase) such that a small repulsive interaction is achieved by electrostatic, solvation, or steric phenomena.

Applying these postulates requires the establishment of special powder forming techniques and careful control of the surface electrochemical properties of the powders. From the fields of controlled precipitation and colloid chemistry, much of the background science can be garnered. The work of Matijevic and coworkers is especially relevant.[14]

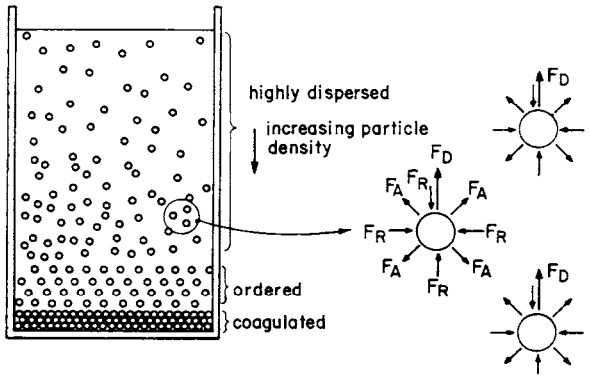

Figure 26.2 Schematic representation of the ordering of monosized particulates from a liquid phase caused by equal drag forces, F_D, and isotropic and equal electrostatic repulsion, F_R, and van der Waals attraction, F_A.

In the following discussion, we show the applicability of these processing concepts to B-doped SiO_2 and doped TiO_2 powders. The synthesis procedures for the spherical, monodisperse doped powders are reviewed. Surface electrochemical properties and dispersion stability of the doped powders are related to the behavior of the pure powders. Finally, the influence of stability and dispersion control on packing and subsequent sintering are discussed.

POWDER SYNTHESIS

The synthesis procedures for the doped powders were derived from those developed for SiO_2[15,16] and TiO_2.[17] The monodisperse, spherical powders were generated through the controlled hydrolysis of dilute alcoholic solutions of the metal alkoxides. The dopants, boron in SiO_2 and Ta, Nb, Ba, Sr, and Cu in TiO_2 were selectively placed either within the particles during the hydrolysis and growth reactions or on the surface after particle formation. The general procedures for pure powder synthesis and dopant incorporation are discussed in the following paragraphs.

B-Doped SiO_2

The single component SiO_2 powders were formed from ethanolic solutions of tetraethylorthosilicate (TEOS), water, and ammonia; typical concentrations were 0.3 *M* TEOS, 4.5 *M* water, and 1.95 *M* ammonia. Powders synthesized under these conditions (T = 298°K) had a mean particle size of 0.5 μm and a log normal σ of 1.05.[16] The basic procedure consisted of adding the desired amounts of water, ammonia, and TEOS, in that order, to the ethanol and mixing, using a magnetic stirrer; particles were detected (in-

creasing turbidity) several minutes after addition of the TEOS and grew to final size within 1 hr.

The addition of B_2O_3 to the SiO_2 powder was desired to enhance densification at reduced temperatures ($\leq$1100°C). Two modes of boron incorporation were available: cohydrolysis of a boron alkoxide and surface precipitation of boric acid.

Since the boron alkoxides hydrolyze more rapidly than TEOS (the rate increases as the alkyl chain length decreases), successful cohydrolysis required the selection of a suitable alkoxide to dope the SiO_2, rather than precipitate B_2O_3. Three boron alkoxides (triethyl, tri-*n*-propyl, and tri-*n*-butyl borate) and several addition methods were tested. The same TEOS, water, and ammonia concentrations used to prepare pure SiO_2 were used in the doping experiments. Since boron was desired near the particle surface, the SiO_2 hydrolysis reaction was initiated and the boron alkoxides were added after 30 min (particles ~ 85% of the final size). Direct addition of the boron alkoxides to the reaction mixture resulted in rapid precipitation of small B_2O_3 particles ($d \leq 0.1$ μm). However, a 5 : 1 dilution (in ethanol) of the propyl and butyl borates and dropwise addition to the mixture gave the desired results. Although the maximum dopant levels achieved were about 1.6 wt.%, the narrow particle size distributions obtained for pure SiO_2 were maintained. An example of a boron doped powder is shown in Fig. 26.3.

Attempts to precipitate boric acid on the particle surface yielded low dopant levels ($\leq$0.4 wt.%) owing to the low solubility of boric acid in water. The precipitation was accomplished by dissolving $B(OH)_3$ in water, adding the solution to a powder sediment cake, and then evaporating the water. This technique, although insufficient by itself, was used to supplement boron addition in powders formed from cohydrolysis.

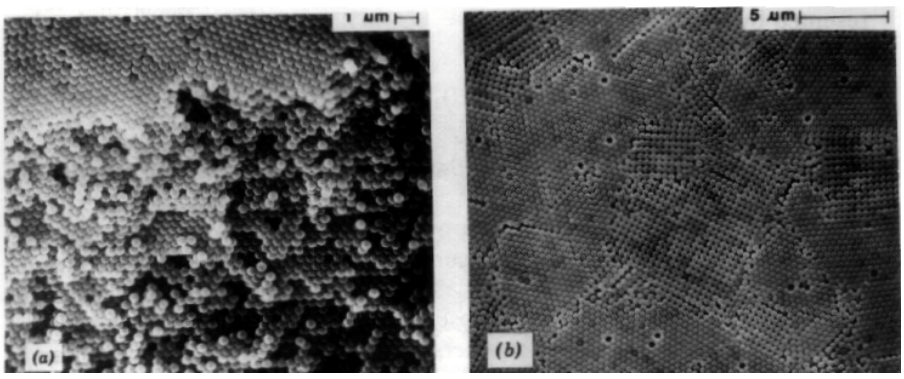

Figure 26.3 Fracture (*a*) and top (*b*) surfaces of a compact formed from monodisperse boron-doped SiO_2.

Doped TiO_2

The pure and doped TiO_2 powders were formed in a water free atmosphere from dilute ethanolic solutions of titanium tetraethoxide and water. The basic procedure consisted of adding a solution of water in ethanol to one of the ethoxide in ethanol and mixing[17]; precipitation was rapid (occurring in 5–60 sec at 25°C). A typical TiO_2 formed using 0.15 *M* ethoxide and 0.5 *M* H_2O had a mean size of 0.4 μm and a log normal σ of 1.12.

The donor dopant (Nb^{5+} or Ta^{5+}) was incorporated uniformly in the particle through cohydrolysis of the metal ethoxide, which had been added to the initial titanium ethoxide/ethanol solution. The overall reaction is described by

$$Ti(OC_2H_5)_4 + M(OC_2H_5)_5 + H_2O \xleftrightarrow{C_2H_5OH} TiO_2 \cdot M_2O_5 \cdot XH_2O \quad (1)$$

where M = Ta or Nb and $X \approx 1$. Reagent concentrations used in the experiments were 0.1 *M* alkoxide and ~0.3–1.5 *M* water; all precipitation reactions were conducted under dry N_2 using 200 proof anhydrous ethanol.

The counter dopant (Ba^{2+}, Sr^{2+}, or Cu^{+}) was placed onto the powder surface after the powder had been washed and redispersed in water. Two methods were employed to dope the surface: inorganic salt precipitation and metal alkoxide hydrolysis. The first method is schematically represented by the general reaction

$$MCl_2(aq) + (NH_4)_2CO_3(aq) = MCO_3 \quad \text{(on particles)} \quad (2)$$

where M = Ba, Sr, or Cu. The metal carbonate, which is deposited on the particle surface, decomposes during sintering (prior to densification) to yield the appropriate metal oxide.

The second method, the metal alkoxide hydrolysis, is schematically represented by the general reaction

$$M(OR)_2 + H_2O = M(OH)_2 \cdot XH_2O \quad \text{(on particle)} \quad (3)$$

where M = Ba or Sr. The metal hydroxide also decomposes on heating to yield either BaO or SrO.

A wide variety of doped titania powders have been prepared using the methods outlined above. Table 26.4 summarizes the dopant combination and chemical composition (dopant level desired) of powders produced. Chemical analyses by plasma emission spectroscopy and instrumental neutron activation analysis indicated that the powders were doped to the desired levels and that dopants were not lost, nor were contaminants added during handling. Figure 26.4 shows a Ta-Sr-doped TiO_2 powder; the spherical shape and the narrow particle size distribution observed for pure TiO_2 were maintained.

Table 26.4 Doped Titania Samples

	Oxide Dopants (Wt.%)				
Sample	Ba	Cu	Nb	Sr	Ta
1	0.2		0.2		
2	0.2		0.5		
3	0.2		0.7		
4	0.2				0.5
5	1.0		1.0		
6	1.0				1.0
7			0.5	0.2	
8			1.0	0.8	
9				0.8	1.0
10			1.0	1.0	
11				1.0	1.0
12		0.2			0.5
13		0.2	0.5		
14					0.1
15			0.1		
16			0.5		
17			1.0		
18					1.0

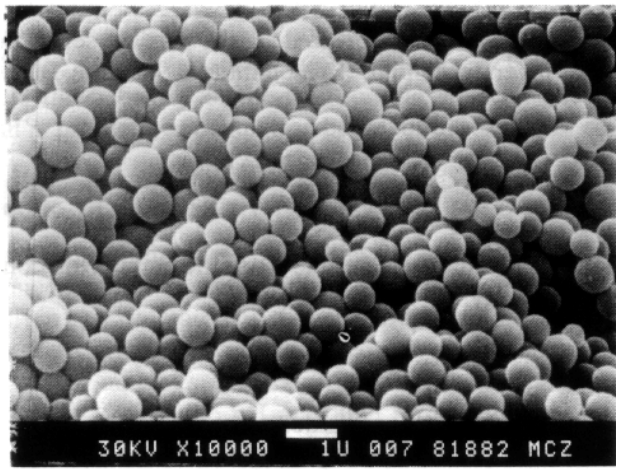

Figure 26.4 Fracture surface of a compact of Sr-Ta-doped TiO_2 (wt. % SrO and 1 wt. % Ta_2O_5).

DISPERSION

Particle Interactions

The state of aggregation of a dispersed powder, which strongly influences powder packing and subsequent sinterability, depends on the stability of the dispersion against coagulation. The approach of two particles, from Brownian motion, sedimentation, or processing forces results in coagulation when the particle interactions are not sufficiently repulsive. The theory describing these interactions (DLVO theory) was recently reviewed.[18,19] The basic equations are given in the following discussion.

The general equation describing the two-body interactions consists of attractive and repulsive terms,

$$V_T = V_A(\text{van der Waals}) + V_R(\text{electrostatic}) + V_R(\text{others}) \tag{4}$$

The van der Waals attraction between two spherical particles of radius a and center-to-center distance r is given by[20]

$$V_A = -\frac{A}{6}\left[\frac{2a^2}{r^2 - 4a^2} + \frac{2a^2}{r^2} + \ln\frac{r^2 + 4a^2}{r^2}\right] \tag{5}$$

where A, the Hamaker constant, depends on the properties of the particles and the dispersion medium ($A \sim 10^{-12}$–10^{-13} ergs). The electrostatic repulsion, arising from the interaction of the electrical double layers surrounding the dispersed particles, has the general form

$$V_R \propto \varepsilon\varepsilon_0\psi_d \exp(-\kappa H) \tag{6}$$

where ε is the medium dielectric constant, H the particle separation, and ψ_d the Stern (diffuse layer) potential. The quantity $1/\kappa$ is the Debye–Huckel length given by

$$1/\kappa = \left(\frac{\varepsilon\varepsilon_0 RT}{F^2 \Sigma_i c_i z_i^2}\right)^{1/2} \tag{7}$$

where F is Faraday's constant, and c_i and z_i are the counterion concentration and valence, respectively.[18]

Coagulation

The rate of coagulation of a dispersion depends on the sign and magnitude of the interaction energies; the frequency of Brownian encounters determines the maximum rate of coagulation in the absence of forces. Coagulation is

retarded by the presence of repulsive interactions, as the maximum repulsive energy ($V_T$max) acts as an activation energy for the process.

Coagulation has been modeled as a biparticle reaction obeying the rate equation

$$\frac{dn}{dt} = -kn^2 \tag{8}$$

where n = particle number density and k = coagulation rate constant. The rate constant for rapid coagulation, based on mutual particle diffusion, was given by Smoluchowski[21] as

$$k_r = 8\pi D n_0 \tag{9}$$

where n_0 is the initial particle concentration and D is the particle diffusion coefficient given by

$$D = kT/6\pi\eta a \tag{10}$$

where η is the dispersion medium viscosity.

The retardation of coagulation owing to repulsive interactions was evaluated in 1934 by Fuchs through the introduction of the stability factor, W, given as

$$W = \frac{k_r}{k_{\text{slow}}} = 2a \int_{2a}^{\infty} \exp\left(\frac{V_T}{kT}\right) \frac{dr}{r^2} \tag{11}$$

where k_{slow} is the rate constant for slow coagulation.[18] Although this theory is restricted to the formation of pairs from primary particles (singlets), stability factors can be experimentally obtained through measurements of the time rate of change of n (or the average particle size). The stability factors not only reveal the behavior of the solution/particle electrochemistry, but are also useful in predicting coagulation behavior in slurries of ceramic powders.

Application to TiO_2 and SiO_2

The two solvent parameters controlling the interaction energy are the electrolyte concentration (c_i, through κ) and the diffuse layer potential (ψ_d) which is often approximated by the measured ζ-potential. The ζ-potential is a strong function of solvent pH and electrolyte concentration, as shown in Fig. 26.5 for an aqueous dispersion of TiO_2 in the presence of KCl. The isoelectric point (IEP), the pH at which no net charge exists in the solid/liquid interface region, is 5.5. Development of a sufficient electrostatic repulsion to prevent coagulation during processing requires control over both

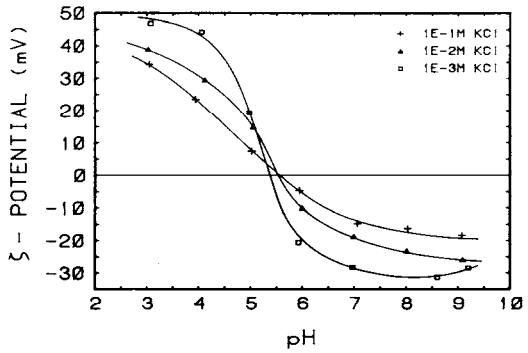

Figure 26.5 Zeta potential of the pure TiO_2 as a function of pH in aqueous KCl solutions (T = 25°C).

electrolyte concentration and pH. Specifically, the pH should be several pH units above or below the IEP, and c_i should be low. The effect of these parameters on stability is shown in Fig. 26.6 (the technique employed to determine W is discussed elsewhere[22]). The primary feature of the data is that the pH range for rapid coagulation (centered about the IEP) increased rapidly as electrolyte concentration was increased.

The ζ-potential versus pH and stability measurements for the SiO_2 powders showed behavior similar to TiO_2, except that IEP is 2.8. Aqueous dispersions formed under basic conditions and $c_i \leq 0.01$ M were found to have a high stability.

Dopant Effects on Stability

The effect of dopant additions to a pure powder on the interfacial electrochemistry and stability depends on the mode of incorporation (surface vs.

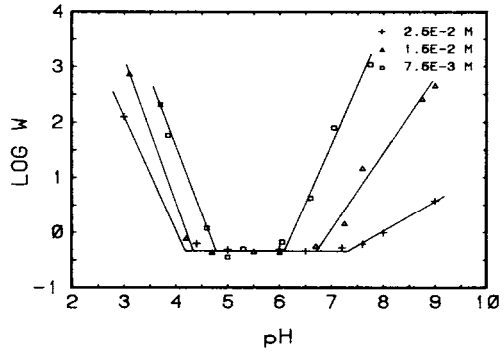

Figure 26.6 Stability ratio of TiO_2 as a function of pH in aqueous KCl solutions (T = 25°C).

bulk), dopant concentration, and the electrochemical properties of the dopant compound. For example, bulk incorporation of a low concentration dopant has little effect on the surface properties, especially when the IEP of the dopant compound is similar to that of the host. However, surface incorporated dopants dramatically alter the electrochemistry when the dopant compound has an appreciably different IEP. For example, B_2O_3 is acidic (IEP $\approx$ 3), and although it is distributed within the outer volume of the SiO_2 particles, the surface properties are not affected. As a result, stable dispersions of the doped SiO_2 were formed under the same conditions (basic solutions) as the pure SiO_2.

The multiply-doped TiO_2 presents a more complicated case. The Nb^{5+} or Ta^{5+} (IEP of oxide $\approx$ 5–7) dopants in the bulk have no effect, whereas the Ba^{2+} counter dopant (or Sr^{2+}) at the surface significantly changes the surface properties. BaO has an IEP of $\approx$12 and $BaTiO_3$ has an IEP $\approx$ 9, thus the presence of Ba^{2+} at the surface, whether in the form of an adsorbed ion or the carbonate, shifts the IEP of the "TiO_2" surface from 5.5 toward 12. Attempts to disperse Ba^{2+} doped powders at pH 9 to 10 were unsuccessful, but a pH $\leq$ 8 yielded stable dispersions.

The affect of Ba^{2+} presence in the TiO_2 double layer is further illustrated in Figs. 26.7 and 26.8. Since Ba^{2+} and Sr^{2+} show strong specific adsorption at the TiO_2/water interface, low concentrations of Ba^{2+} caused charge reversal and "BaO-like" behavior, as shown by the electrophoresis data in Fig. 26.7. Figure 26.8, showing the measured stability factor of TiO_2 in the presence of Ba^{2+}, confirms the adsorption behavior. Similar specific adsorption of Ba^{2+}, and other alkaline earth cations (Mg^{2+}, Ca^{2+}, and Sr^{2+}), on TiO_2 was observed by Fuernstenau.[23] Furthermore, the effect of cation charge (through κ) is evident; instability occurs at much lower cation concentrations than for KCl. This example illustrates that dispersion stability is very sensitive to the presence of impurities and dopants, thus their existence must be controlled and their effects must be understood.

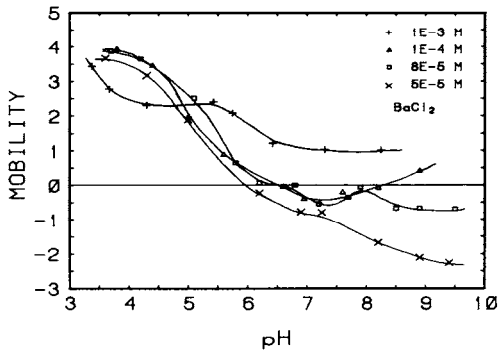

Figure 26.7 Electrophoretic mobility of TiO_2 in aqueous $BaCl_2$ solutions (T = 25°C).

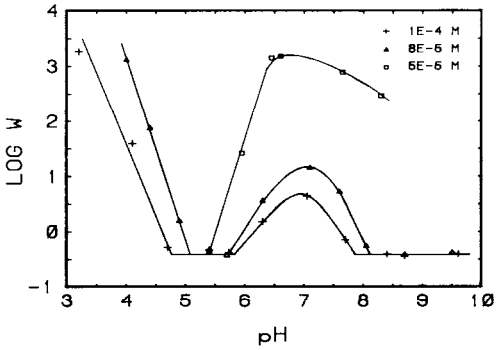

Figure 26.8 Stability ratio of TiO_2 as a function of pH in aqueous $BaCl_2$ solutions (T = 25°C).

PACKING AND SINTERING

To achieve reliability and reproducibility in ceramics processing, uniformly-packed green microstructures must be obtained. Uniform particle packing, the consequence of a stable dispersion of uniform-size powder, not only influences sinterability, but also results in uniform, controlled shrinkages. Although these concepts were proved valid for pure TiO_2[17], difficulties remain in general applications, primarily because of the lack of understanding of the phenomena that occur during the final processing steps. As a specific example, when dispersed sediments or casts (particles not touching) are dried, nonuniform shrinkages result in fractures within the compact, which translates to the loss of structural integrity during firing.

A plausible explanation for this phenomenon was formulated and techniques based on the explanation were successfully employed in forming sinterable compacts. The problem arises from the separation (by design) of particles in the dispersed sediment resulting from the repulsive electrostatic forces. The volume of the sediment is thus defined by the average interparticle separation. As solvent is removed from the cast, particle adhesion to container walls and nonuniform drying result in tensile stresses sufficient to overcome van der Waals forces, and hence cause cracks in the dried body.

To eliminate the cracking problem, external forces (chemical, mechanical, or electrical) must be applied to overcome the repulsive force and collapse the dispersed sediment (cast) into a compact sediment (greenware). This uniform reduction in the cast volume leads to lower drying shrinkage and stresses, thereby significantly reducing (or eliminating) cracking.

The application of external forces was successful for several systems.[24] Addition of salts (chemical force) to dispersed sediments of TiO_2 resulted in the collapse of the double layer (recall the effect of c_i on ζ and κ), and mechanical (doctor blade) and electrical (electrophoretic deposition) forces were successful in preliminary film casting (15–40 μm thick) experiments for Al_2O_3 and $BaTiO_3$.

The boron-doped SiO_2 also suffered from the adhesion and drying problems; acceptable green compacts (from sedimentation) were difficult to obtain and those that were sintered cracked severely. This problem was especially prevalent in thin film (<100 μm thick) casting experiments, as shown in Fig. 26.9. The use of binder (PVA) improved green strength, but degraded particle packing. Again, sintering gave unacceptable results. However, thin compacts (~500 μm thick) having a green density of about 65% of theoretical were successfully prepared, without using a binder or external forces, and were sintered to nearly theoretical density in 1 hr at 1000°C (Fig. 26.10).

Large compacts (>0.5 cm thick) were obtained by forced (chemical) compaction of the dispersed sediment with addition of a concentrated aqueous solution of boric acid and NaCl; dense, uniform packing of particles was achieved (Fig. 26.3). These green compacts ($\rho \approx 70\% \rho_{th}$) readily sintered to near full density. Figure 26.11 shows the top and fracture surfaces of a compact sintered for 2 hr at 1050°C.

Dense, uniform compacts of doped TiO_2 powders were generally not obtained in initial experiments. Since the electrochemical properties of the particle/solution interface were not understood, stable dispersions were difficult to obtain; particles usually coagulated during sedimentation, resulting in low density compacts. However, the recent study of adsorbed Ba^{2+} on TiO_2, previously discussed, led to the formation of stable dispersions in neutral (pH $\approx$ 7) aqueous solutions. Figure 26.12 shows the top surface of a compact

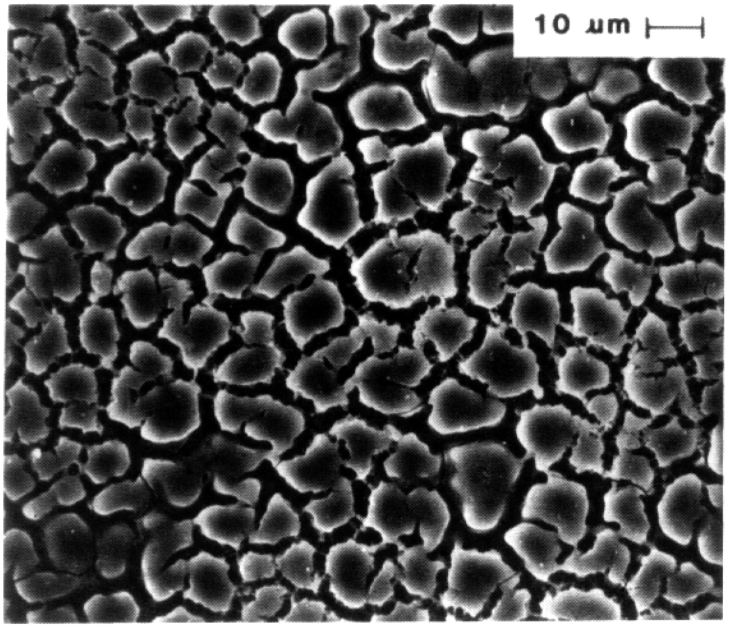

Figure 26.9 SEM of a 5 μm film of B-doped SiO_2 particles sintered at 1000°C for 5 hr.

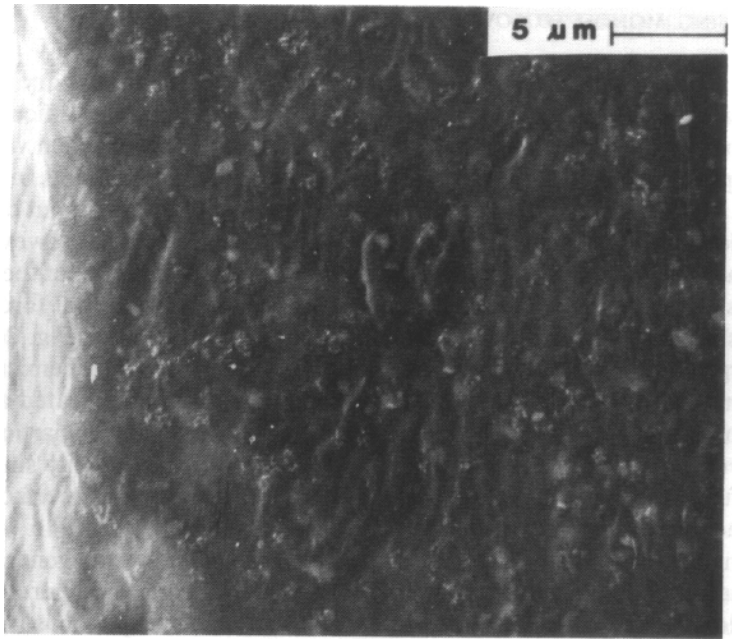

Figure 26.10 SEM showing the surface of a thin cake of B-doped SiO_2 sintered at 1000°C for 1 hr.

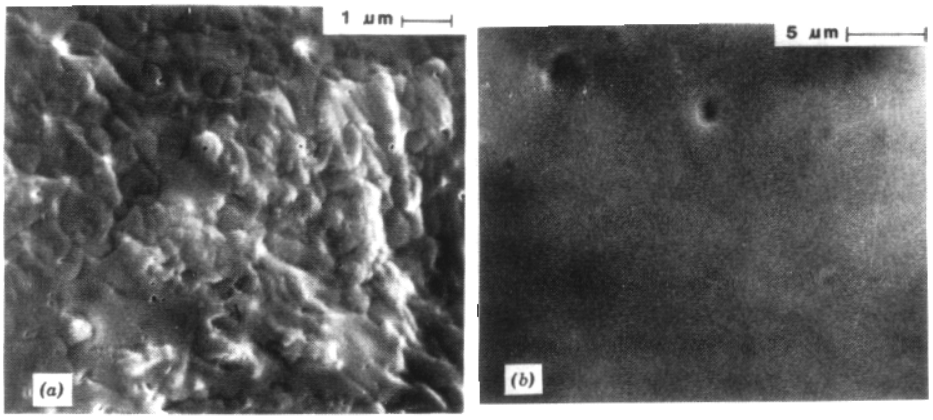

Figure 26.11 SEM of B-doped SiO_2 particles coated with boric acid and NaCl and sintered at 1050°C for 2 hr: (*a*) top surface and (*b*) fracture surface.

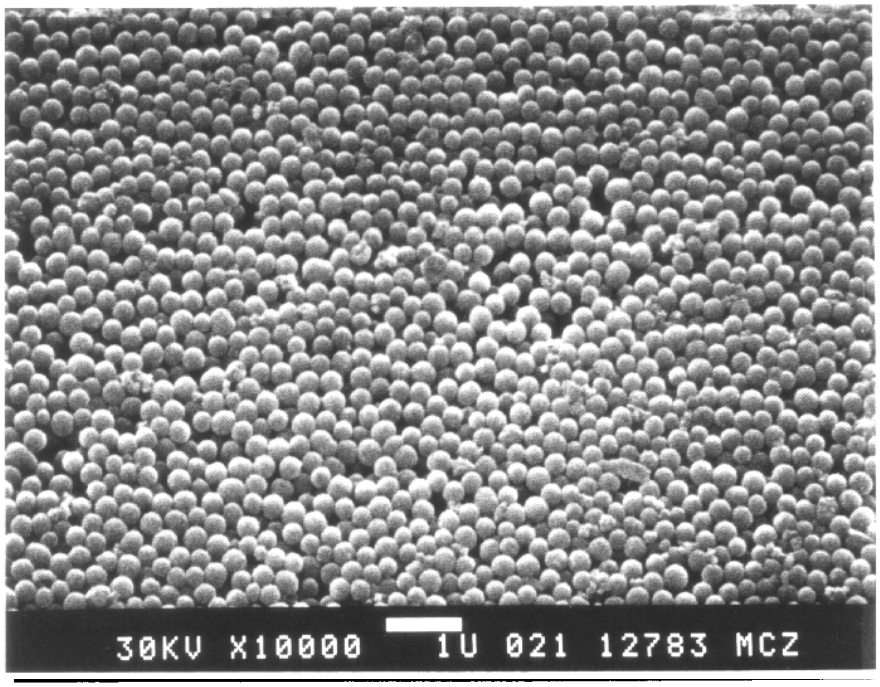

Figure 26.12 Top surface of a compact of Ba-Nb-doped TiO_2 (0.2% BaO and 0.5% Nb_2O_5).

formed from Ba-Nb-doped TiO_2, and Fig. 26.4 shows the fracture surface of a compact formed from Sr-Ta-doped TiO_2. Sintering behavior of these compacts has not yet been investigated; however, experience indicates that rapid densification should occur for these compacts at ~1100°C.

CONCLUSIONS

Ultrastructure processing of crystalline ceramics begins with the controlled formation of powders, which already contain elements of the desired structure, and continues through controlled particle packing to densification. In this chapter, we demonstrated these features in the synthesis of powders for pure and doped oxide systems. We also outlined the critical parameters to be studied and controlled when reliable powder processing (dispersion and packing) is required. The distinct advantages of using monosized, unagglomerated powders that are processed from liquid media to produce green microstructures of uniformly packed particulates were demonstrated. Finally, the preliminary sintering studies indicate that uniform, fine-grained, dense microstructures can be produced at substantially lower temperatures.

ACKNOWLEDGMENTS

The authors acknowledge support for this research from the Department of Energy, IBM, American Electric Power, and Bonneville Power Authority.

REFERENCES

1. H. K. Bowen et al., "Basic Needs in High Temperature Ceramics," *J. Mater. Sci. Eng.* **44,** 1–56 (1980).
2. G. B. Kenney and H. K. Bowen, "High Tech Ceramics in Japan: Current and Future Markets," *Bull. Am. Ceram. Soc.* **62,** 590–596 (1983).
3. G. C. Kuczynski, "Self-Diffusion in Sintering of Metallic Particles," *Trans. AIME* **185,** 169 (1949).
4. Consider two examples from the General Electric Laboratory: R. L. Coble, "Transparent Alumina and Method of Preparation," U.S. Patent No. 3,026,210, March 20, 1962; and S. Prochaska, in *Ceramics for High-Performance Applications,* Brook Hill Massachusetts, 1974, pp. 239–252.
5. See the work of C. Greskovich and K. Lay, reported in W. D. Kingery et al., *Introduction to Ceramics,* Wiley, New York, 1975, pp. 481–484; or in *Processing of Crystalline Ceramics,* Plenum Press, New York, 1978; also see papers by M. D. Sacks and J. A. Pask, "Sintering of Mullite," pp. 193–204 and J. S. Reed et al., "Some Effects of Aggregates and Agglomerates in the Fabrication of Fine Ceramics," pp. 171–180.
6. M. Yan, in *Advances in Powder Technology,* G. Chin, Ed., ASM, Ohio, 1982, pp. 99–133.
7. K. S. Mazdiyasni et al., "Preparation of Ultra-High-Purity Submicron Refractory Oxides," *J. Am. Ceram. Soc.* **48,** 372–375 (1965).
8. W. H. Rhodes, "Agglomeration and Particle Size Effects on Sintering Yttria-Stabilized Zirconia," *J. Am. Ceram. Soc.* **64,** 19–22 (1981).
9. W. D. Kingery and M. Berg, "Study of the Initial Stages of Sintering Solids by Viscous Flow, Evaporation-Condensation, and Self-Diffusion," *J. Appl. Phys.* **26,** 1205 (1955).
10. R. M. Cannon, private communication.
11. See R. M. Cannon and R. L. Coble, in *Processing of Crystalline Ceramics,* H. Palmour III et al., Eds., Plenum Press, New York, 1978, pp. 151–170; M. F. Yan, R. M. Cannon, and H. K. Bowen, in *Ceramic Microstructures 76,* R. M. Fulrath and J. A. Pask, Eds., Westview Press, Colorado, 1977, pp. 276–307; M. F. Man, R. M. Cannon, H. K. Bowen, and U. Chowdhry, "Effect of Grain Size Distribution on Sintered Density," Report #7, MIT Ceramics Processing Research Lab., October 1980, *Mater. Sci. and Eng.* **60,** 275–281 (1983).
12. A. Kose et al., "Direct Observation of Ordered Latex Suspensions by Metallurgical Microscopy," *J. Colloid Interface Sci.* **44,** 330–338 (1973); R. K. Iler, "Formation of Precious Opal," *Nature* **207,** 472–473 (1965).
13. W. D. Cooper, "Coagulation of Polydisperse Colloidal Systems," *Kolloid. z.z. Polym.* **250,** 38–45 (1972); M. Strauss, T. Ring, A. Bleier, and H. K. Bowen,

"Effect of Particle Size Distribution Effects and Processing Ceramic Suspension," submitted to *J. Am. Ceram. Soc.*

14. E. Matijevic, "Preparation and Characterization of Monodispersed Metal Hydrous Oxide Sols," *Prog. Colloid Polym. Sci.* **61,** 24–35 (1976).
15. W. Stoeber, A. Fink, and E. Bohn, "Controlled Growth of Monodisperse Silica Spheres in the Micron Size Range," *J. Colloid Interface Sci.* **26,** 62–69 (1968).
16. C. Huynh, Ph.D. Thesis, MIT, 1984.
17. E. A. Barringer and H. K. Bowen, "Formation, Packing and Sintering of Monodisperse TiO_2 Powders," *J. Am. Ceram. Soc.* **65,** C199–C201 (1982).
18. J. Th. G. Overbeek, "Recent Developments in the Understanding of Colloid Stability," *J. Colloid Interface Sci.* **58,** 408–422 (1977).
19. R. H. Ottewill, "Stability and Instability in Disperse Systems," *J. Colloid Interface Sci.* **58,** 357–373 (1977).
20. H. C. Hamaker, *Physica* **4,** 1058 (1937).
21. M. Von Smoluchowski, *Phys. Z.* **17,** 593 (1916).
22. E. Barringer, B. Novich, and T. Ring, "Colloid Stability Determination for Oxide Powders Using Photon Correlation Spectroscopy," submitted to *J. Colloid Interface Sci.*
23. D. W. Fuerstenau, D. Manmohan, and S. Raghavan, in *Adsorption from Aqueous Solutions,* Plenum Press, New York, 1981, pp. 93–117.
24. R. L. Pober, E. A. Barringer, M. V. Parish, N. Levoy, and H. K. Bowen, "Dispersion and Packing of Narrow Size Distribution Ceramic Powders," *Proceedings 19th University Conference on Ceramic Science,* Nov. 1982, North Carolina State University.